Time integration in solid mechanics

From asymptotics to conservation principles

Krenk, Steen

Published in:
Proceedings of the 20th Nordic Seminar on Computational Mechanics

Publication date:
2007

Document Version
Publisher's PDF, also known as Version of record

Time Integration in Solid Mechanics.
From Asymptotics to Conservation Principles

Steen Krenk
Department of Mechanical Engineering.
Technical University of Denmark, Lyngby, Denmark
e–mail: sk@mek.dtu.dk

Introduction

Numerical time integration of mechanical systems is used in many applications in civil and structural engineering, modelling of engines and other rotating machinery as well as in robotics. Traditionally the numerical integration has been carried out by reformulating the appropriate differential equations to difference equations for finite time increments by substituting Taylor expansion representations. While these methods often work well for unconstrained linear problems, problems are often encountered for strongly non-linear problems, e.g. in connection with moving bodies, and when implementing constraints, e.g. via Lagrange multipliers.

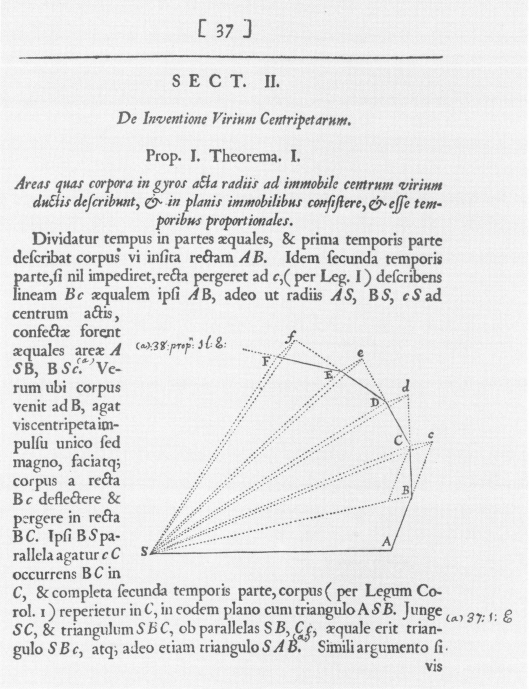

[37]

SECT. II.

De Inventione Virium Centripetarum.

Prop. I. Theorema. I.

Areas quas corpora in gyros acta radiis ad immobile centrum virium ductis describunt, & in planis immobilibus consistere, & esse temporibus proportionales.

Dividatur tempus in partes æquales, & prima temporis parte describat corpus vi insita rectam *AB*. Idem secunda temporis parte, si nil impediret, recta pergeret ad *c*, (per Leg. I) describens lineam *Bc* æqualem ipsi *AB*, adeo ut radiis *AS*, *BS*, *cS* ad centrum actis, confectæ forent æquales areæ *ASB*, *BSc*. (a) Verum ubi corpus venit ad B, agat vis centripeta impulsu unico sed magno, faciatq; corpus a recta *Bc* deflectere & pergere in recta *BC*. Ipsi *BS* parallela agatur *cC* occurrens *BC* in *C*, & completa secunda temporis parte, corpus (per Legum Corol. 1) reperietur in *C*, in eodem plano cum triangulo *ASB*. Junge *SC*, & triangulum *SBC*, ob parallelas *SB*, *Cc*, æquale erit triangulo *SBc*, atq; adeo etiam triangulo *SAB*. Simili argumento si vis

(a) 38. prop. 1. L.

(a) 37. 1. &

Figure 1: Incremental development of linear momentum, Principia (1686)

A different type of time integration algorithms has been developed over the last 15-20 years, based on an integrated form of the equations of motion. The basic idea can be illustrated with reference to the famous momentum diagram from Newton's Principia [1]. Loosely stated the equation of motion can be given in the form of a differential equation, or its integrated momentum form,

$$\frac{d}{dt}\big(\,m\,\mathbf{v}\big) \;=\; \mathbf{f}(r) \qquad , \qquad \big[\,m\,\mathbf{v}\big]_{\Delta t} \;=\; \int_{\Delta t} \mathbf{f}(r)\,d\tau \tag{1}$$

In the classic approach the differential on the left side of the equation of motion is represented by an approximate difference expression, while in the momentum-based methods the integrated form is used, and the approximation lies in the representation of the force integral. In Newton's figure the momentum increment is the development from Bc to BC, and the difference cC is the force integral. The momentum increment approach enables exact representation of certain conservation theorems, e.g. for momentum and energy for single or multiple particles, see [2, 3]. A general survey of conservation type integration methods has been given by Hairer et al. [4]. However, a number of special procedures have been developed for time integration of large motion of deformable solid bodies, and a survey of some of these is presented in the following.

Geometric stiffness in conservation algorithms

Consider a body with displacement vector $\mathbf{u}$ and internal forces given in terms of a potential function as $\mathbf{g}(\mathbf{u}) = \boldsymbol{\nabla}_{\mathbf{u}} G(\mathbf{u})$, where $\boldsymbol{\nabla}_{\mathbf{u}}$ denotes the derivatives with respect to $\mathbf{u}$. The equation of motion to be considered is of the form

$$\mathbf{M}\ddot{\mathbf{u}}(t) + \mathbf{C}\dot{\mathbf{u}}(t) + \boldsymbol{\nabla}_{\mathbf{u}} G(\mathbf{u}) \;=\; \mathbf{f}(t) \tag{2}$$

where $\mathbf{f}(t)$ is the load vector, and $\mathbf{C}$ is a matrix representing linear viscous damping.

The energy balance equation corresponding to the equation of motion (2) is obtained from multiplication with $\dot{\mathbf{u}}^T$, followed by integration,

$$\frac{d}{dt}\Big(\tfrac{1}{2}\dot{\mathbf{u}}^T\mathbf{M}\dot{\mathbf{u}} \,+\, G(\mathbf{u}) \Big) \;=\; \dot{\mathbf{u}}^T\mathbf{f} \,-\, \dot{\mathbf{u}}^T\mathbf{C}\dot{\mathbf{u}} \tag{3}$$

The relation between the potential in the energy balance equation and the internal force vector in the equation of motion follows from application of the 'chain rule' of differentiation as

$$\frac{d}{dt} G(\mathbf{u}) \;=\; \dot{\mathbf{u}}^T\, \boldsymbol{\nabla}_{\mathbf{u}} G(\mathbf{u}) \tag{4}$$

The key to energy conservation is to develop an algorithm that contains the equivalent relation for a finite time interval and thereby a finite displacement increment $\Delta\mathbf{u}$.

The second order differential equation of motion (2) is recast into state-space format by introducing the independent velocity variable $\mathbf{v} = \dot{\mathbf{u}}$. When this definition is multiplied by the mass matrix $\mathbf{M}$ the augmented system for the state-space variables $[\,\mathbf{u}, \mathbf{v}\,]$ can be given in the following symmetric form,

$$\begin{bmatrix} \mathbf{C} & \mathbf{M} \\ \mathbf{M} & \mathbf{0} \end{bmatrix} \begin{bmatrix} \dot{\mathbf{u}} \\ \dot{\mathbf{v}} \end{bmatrix} + \begin{bmatrix} \boldsymbol{\nabla}_{\mathbf{u}} G(\mathbf{u}) \\ -\mathbf{M}\,\mathbf{v} \end{bmatrix} = \begin{bmatrix} \mathbf{f}(t) \\ \mathbf{0} \end{bmatrix} \tag{5}$$

The purpose of a single step time integration is to advance the state-space variables $\mathbf{u}$ and $\mathbf{v}$ from time t_n to t_{n+1}. Therefore the equations are integrated over the time interval $[t_n, t_{n+1}]$.

$$\begin{bmatrix} \mathbf{C} & \mathbf{M} \\ \mathbf{M} & \mathbf{0} \end{bmatrix} \begin{bmatrix} \Delta\mathbf{u} \\ \Delta\mathbf{v} \end{bmatrix} + \begin{bmatrix} \int \boldsymbol{\nabla}_{\mathbf{u}} G(\mathbf{u})\, dt \\ -\mathbf{M} \int \mathbf{v}\, dt \end{bmatrix} = \begin{bmatrix} \int \mathbf{f}(t)\, dt \\ \mathbf{0} \end{bmatrix} \tag{6}$$

The time integral of the external force is represented as the interval length Δt times the arithmetic mean of the end-point values $\bar{\mathbf{f}}$, and the velocity integral is similarly represented as $\Delta t\, \bar{\mathbf{v}}$.

The material is now assumed to be linear elastic in terms of the Green strain tensor $\mathbf{E}$ and the second Piola-Kirchhoff stress tensor $\mathbf{S}$. This implies the linear relation $\mathbf{S} = \mathbf{D}\mathbf{E}$ where $\mathbf{D}$ is the constant stiffness tensor. When using the fact that the Green strain is a quadratic function of the displacement gradient it can be demonstrated that the increment of the internal energy takes the form

$$\big[\, G(\mathbf{u}) \,\big]_n^{n+1} \;=\; \Delta\mathbf{u}^T \int_{V_0} (\overline{\boldsymbol{\nabla}_{\mathbf{u}} \mathbf{E}^T})\; \bar{\mathbf{S}}\; dV_0 \tag{7}$$

This is a finite increment form of (4) and an exact integral is therefore obtained, when the internal force is represented by the integral of the mean value product. This was originally shown by Simo & Tarnow [5] for linear elasticity, and extended to more general material models by Gonzalez [6]. It has later been demonstrated [7], that the internal force as defined by the integral in (7) can be expressed as the mean value of the internal force at the end-points of the integration interval, minus a correction term,

$$\mathbf{g}_* \;=\; \tfrac{1}{2}\big[\, \mathbf{g}_{n+1} + \mathbf{g}_n \,\big] \;-\; \tfrac{1}{4}\Delta\mathbf{K}^g\, \Delta\mathbf{u} \tag{8}$$

where $\Delta\mathbf{K}^g$ is the increment of the geometric stiffness matrix, usually available in finite element programs.

Algorithmic high-frequency dissipation

The energy equation corresponding to the discretized equations derived in the previous section can be expressed in the form

$$\big[\, \tfrac{1}{2}\mathbf{v}^T\mathbf{M}\,\mathbf{v} + \tfrac{1}{2}\mathbf{u}^T\mathbf{K}\,\mathbf{u} \,\big]_n^{n+1} \;=\; \Delta\mathbf{u}^T\bar{\mathbf{f}} \;-\; \Delta\mathbf{u}^T\mathbf{C}\,\Delta\mathbf{u} \tag{9}$$

This is quite similar in form to the energy balance equation (3). However, a frequency analysis of the algorithm reveals that for discrete time increments Δt the damping effect from a viscous damping matrix $\mathbf{C}$ vanishes for high frequency response.

It is desirable to have a controllable damping of he high-frequency response components, as these are often of spurious nature due to errors introduced by spatial discretization in the form of elements. This can be obtained by introducing balanced terms in both of the state space equations [8, 9]

$$\begin{bmatrix} \mathbf{C}+\frac{1}{2}\alpha h\mathbf{K} & \mathbf{M} \\ \mathbf{M} & -\frac{1}{2}\alpha h\mathbf{M} \end{bmatrix} \begin{bmatrix} \Delta\mathbf{u} \\ \Delta\mathbf{v} \end{bmatrix} + \begin{bmatrix} \mathbf{K} & \mathbf{0} \\ \mathbf{0} & -\mathbf{M} \end{bmatrix} \begin{bmatrix} \Delta t\,\bar{\mathbf{u}} \\ \Delta t\,\bar{\mathbf{v}} \end{bmatrix} = \begin{bmatrix} \Delta t\,\bar{\mathbf{f}} \\ \mathbf{0} \end{bmatrix} \tag{10}$$

The algorithmic dissipation is controlled by the non-dimensional parameter α. In the absence of viscous damping the corresponding energy balance equation is

$$\big[\, \tfrac{1}{2}\mathbf{v}^T\mathbf{M}\,\mathbf{v} + \tfrac{1}{2}\mathbf{u}^T\mathbf{K}\,\mathbf{u} \,\big]_n^{n+1} \;=\; \Delta\mathbf{u}^T\bar{\mathbf{f}} \;-\; \tfrac{1}{2}\alpha\Big(\Delta\mathbf{u}^T\mathbf{K}\,\Delta\mathbf{u} \;-\; \Delta\mathbf{v}^T\mathbf{M}\,\Delta\mathbf{v}\Big) \tag{11}$$

It is seen that the dissipation term has the same form as the energy, but with the state space variables $[\mathbf{u}, \mathbf{v}]$ replaced by their increments $[\Delta\mathbf{u}, \Delta\mathbf{v}]$ over the finite time increment Δt.

The low-frequency algorithmic damping ratio is given in terms of the parameter α and the non-dimensional frequency $\Omega = \omega\Delta t$, where ω is the modal frequency of the structure,

$$\zeta \;=\; \tfrac{1}{2}\alpha\,\Omega\,\big[\, 1 \;+\; \mathrm{O}(\Omega^2) \,\big] \tag{12}$$

It is seen that the algorithmic damping ratio increases linearly with the natural frequency, and thus this type of algorithmic does not leave the low-frequency response unaffected as intended. The

damping characteristics are conveniently represented in terms of the amplification factor λ which is the (complex) factor that propagates the modal state-space response one time increment. The amplification factor of the scheme (10) is shown as dashed curves in Fig. 2.

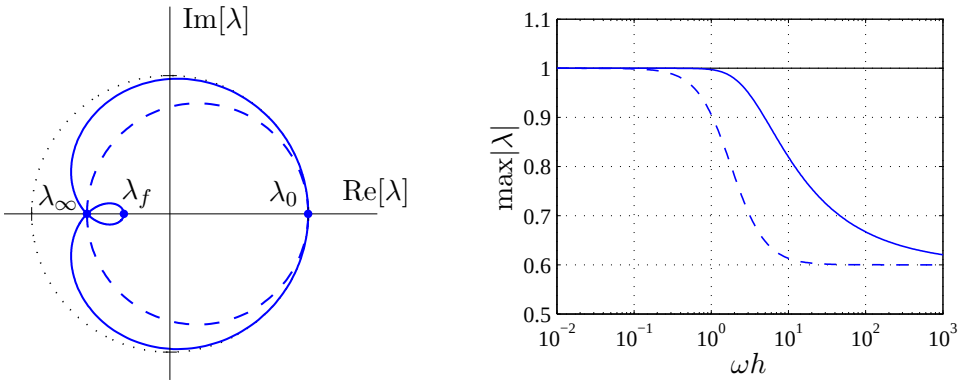

Figure 2: Algorithmic damping with $|\lambda_\infty| = 0.6$. a) Amplification factor λ, b) Spectral radius $|\lambda|_{\max}$.

It has recently been shown that improved low-frequency damping properties can be obtained by changing the mechanism of the algorithmic damping [9]. In the balanced dissipation algorithm (10) the energy dissipation is introduced via the diagonal terms containing $\Delta\mathbf{u}$ and $\Delta\mathbf{v}$. In the low and mid-frequency regime these terms are roughly equivalent to $\Delta t\dot{\mathbf{u}}$ and $\Delta t\dot{\mathbf{v}}$. The idea is to replace these terms formulated by use of the state-space variables with similar terms using a new set of variables $\mathbf{s}(t)$ and $\mathbf{t}(t)$ defined via first order filters with scalar coefficients,

$$\alpha\Delta t\,\dot{\mathbf{s}} + \mathbf{s} = \Delta t\,\dot{\mathbf{u}} \qquad , \qquad \alpha\Delta t\,\dot{\mathbf{t}} + \mathbf{t} = \Delta t\,\dot{\mathbf{v}} \tag{13}$$

where $\alpha\Delta t$ defines the attenuation time of the filter. The resulting algorithm takes the form of the state-space equations

$$\begin{bmatrix} \mathbf{C} & \mathbf{M} \\ \mathbf{M} & \mathbf{0} \end{bmatrix} \begin{bmatrix} \Delta\mathbf{u} \\ \Delta\mathbf{v} \end{bmatrix} + \Delta t \begin{bmatrix} \mathbf{K} & \mathbf{0} \\ \mathbf{0} & -\mathbf{M} \end{bmatrix} \begin{bmatrix} \bar{\mathbf{u}} \\ \bar{\mathbf{v}} \end{bmatrix} + \tfrac{1}{4}\alpha^2\Delta t \begin{bmatrix} \mathbf{K} & \mathbf{0} \\ \mathbf{0} & -\mathbf{M} \end{bmatrix} \begin{bmatrix} \Delta\mathbf{s} \\ \Delta\mathbf{t} \end{bmatrix} = \Delta t \begin{bmatrix} \bar{\mathbf{f}} \\ \mathbf{0} \end{bmatrix} \tag{14}$$

supplemented by the discretized filter equations

$$\alpha \begin{bmatrix} \Delta\mathbf{s} \\ \Delta\mathbf{t} \end{bmatrix} + \begin{bmatrix} \bar{\mathbf{s}} \\ \bar{\mathbf{t}} \end{bmatrix} = \begin{bmatrix} \Delta\mathbf{u} \\ \Delta\mathbf{v} \end{bmatrix} \tag{15}$$

The energy balance relation of this algorithm without viscous damping is

$$\begin{aligned} \big[\, \tfrac{1}{2}\mathbf{v}^T\mathbf{M}\,\mathbf{v} + \tfrac{1}{2}\mathbf{u}^T\mathbf{K}\,\mathbf{u} + \tfrac{1}{8}\alpha^2\big(\mathbf{t}^T\mathbf{M}\,\mathbf{t} + \mathbf{s}^T\mathbf{K}\,\mathbf{s}\big)\,\big]_n^{n+1} \;=& \\ \Delta\mathbf{u}^T\bar{\mathbf{f}} \;-\; \tfrac{1}{4}\alpha^3\big(\Delta\mathbf{s}^T\mathbf{K}\,\Delta\mathbf{s} \;+\; \Delta\mathbf{t}^T\mathbf{M}\,\Delta\mathbf{t}\big)& \end{aligned} \tag{16}$$

It is seen that the dissipation now only depends on the auxiliary variables $[\mathbf{s}, \mathbf{t}]$. This removes the low frequency damping, and leads to the algorithmic damping ratio

$$\zeta \;=\; \tfrac{1}{4}\alpha^3\,\Omega^3\,\big[\,1 + \mathrm{O}(\Omega^2)\,\big] \tag{17}$$

proportional to the third power of the frequency. The two algorithms with built in algorithmic damping lead to monotonous decay of free vibrations, and avoid the spurious oscillations associated with collocation type algorithms, [9].

Moving frame of reference

Modelling of rotating bodies introduce new problems associated with the non-commutativity of rotations, see e.g. [10]. The problem, as well as an effective numerical procedure, is here illustrated with reference to a rigid body with local inertial tensor $\mathbf{J}$, local angular velocity $\boldsymbol{\Omega}$, and instantaneous orientation defined by the rotation tensor $\mathbf{R}_n$. The local equation of motion is

$$\mathbf{J}\,\frac{d\boldsymbol{\Omega}}{dt} + \widehat{\boldsymbol{\Omega}}\,\mathbf{J}\,\boldsymbol{\Omega} = \mathbf{M} \tag{18}$$

In a time increment $[t_n, t_{n+1}]$ the body rotates further by the local angular 'vector' $\boldsymbol{\Phi}$. A momentum and energy conserving scheme was set up for this problem by Simo & Wong [11] consisting of a discretized form of the equation of motion (18) and a relation between the incremental angle $\boldsymbol{\Phi}$ and the angular velocity $\boldsymbol{\Omega}$. It turns out to be convenient to represent the incremental rotation in terms of the Cayley vector

$$\boldsymbol{\Psi} = \frac{1}{\varphi}\tan(\tfrac{1}{2}\varphi)\,\boldsymbol{\Phi} \tag{19}$$

with the associated representation of the incremental rotation tensor

$$\mathbf{R}(\boldsymbol{\Psi}) = (\mathbf{I} - \widehat{\boldsymbol{\Psi}})^{-1}(\mathbf{I} + \widehat{\boldsymbol{\Psi}}) \tag{20}$$

By use of this representation the angular moment balance leading to (18) can be expressed *directly* as [12],

$$\mathbf{J}\,\Delta\boldsymbol{\Omega} + 2\widehat{\boldsymbol{\Psi}}\,\mathbf{J}\,\overline{\boldsymbol{\Omega}} = \big(\overline{\mathbf{M}} + \tfrac{1}{2}\widehat{\boldsymbol{\Psi}}\,\Delta\mathbf{M}\big)\Delta t \tag{21}$$

where $\widehat{\boldsymbol{\Psi}} = \boldsymbol{\Psi}\times$ represents the shew-symmetric component matrix associated with the vector components. The corresponding discretized form of the angular velocity relation is

$$\boldsymbol{\Phi} = \big[(\tfrac{1}{2}+\alpha)\,\boldsymbol{\Omega}_{n+1} + (\tfrac{1}{2}-\alpha)\,\boldsymbol{\Omega}_n\big]\,\Delta t \tag{22}$$

where $\alpha = 0$ corresponds to energy conservation, while $\alpha > 0$ leads to energy dissipation [12].

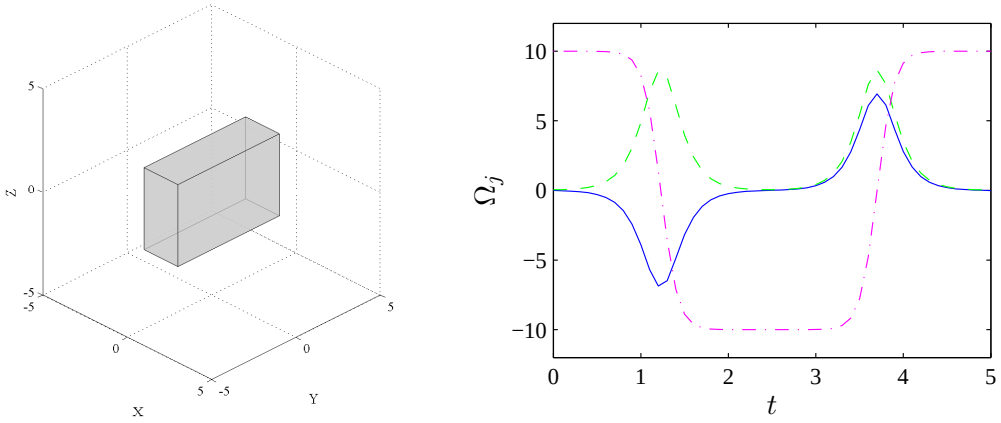

Figure 3: Local angular velocity components for $\Delta t = 0.1$: Ω_1 (—), Ω_2 (- -), Ω_3 (-·-).

Figure 3 shows the undamped whirling motion of a box with side lengths [1,3,2] and mass 12. The intermediate axis is vertical and the box is started spinning with $\boldsymbol{\Omega} = [0.0, 0.05, 10.0]$, corresponding to a small deviation from the intermediate axis. The algorithm is very effective with only about 2.5 iterations for a relative error of 10^{-6}, and reproduces the well known tilting behavior.

Concluding remarks

Some of the main points of the new generation of conservation time integration procedures have been illustrated. An important additional aspect, which can not be covered here is the fact that momentum and energy conserving algorithms can include constraints in terms of Lagrange multipliers, [13, 14, 15]. This removes the numerical problems with spurious oscillations typically associated with Langrange multipliers when using collocation methods.

References

[1] I. Newton. *Philosophiae Naturalis Principia Mathematica*. London, (1686).

[2] R.A. LaBudde, D. Greenspan. Energy and momentum conserving methods of arbitrary order for the numerical integration of equations of motion. I. Motion of a single particle. *Numer. Math.*, **25**, 323–346, (1976).

[3] R.A. LaBudde, D. Greenspan. Energy and momentum conserving methods of arbitrary order for the numerical integration of equations of motion. II. Motion of a system of particles. *Numer. Math.*, **26**, 1–16, (1976).

[4] E. Hairer, C. Lubich, G. Wanner. *Geometric Numerical Integration, Structure-Preserving Algorithms for Ordinary Differential Equations*, 2nd ed. Springer, Berlin , (2006).

[5] J.C. Simo, N. Tarnow. The discrete energy-momentum method. Conserving algorithms for nonlinear elastodynamics. *Zeitschrift für angewandte Mathematik und Physik*, **43**, 757–792, (1992).

[6] O. Gonzalez. Exact energy and momentum conserving algorithms for general models in non-linear elasticity. *Computer Methods in Applied Mechanics and Engineering* 2000; **190**:1763–1783.

[7] S. Krenk. The role of geometric stiffness in momentum and energy conserving time integration. *Int. J. Numer. Meth. Engng.*, **71**, 631–651, (2007).

[8] Armero F, Romero I, On the formulation of high-frequency dissipative time-stepping algorithms for nonlinear dynamics. Part II: Second order methods. *Computer Methods in Applied Mechanics and Engineering*, **190**, 6783–6824, (2001).

[9] S. Krenk. Extended state-space time itegration with high-frequency energy dissipation. *Int. J. Numer. Meth. Engng.*, (in press).

[10] M. Geradin, A. Cardona. *Flexible Multibody Dynamics. A Finite Element Approach*. Wiley, Chichester, U.K., 2001.

[11] J.C. Simo, K.K. Wong. Unconditionally stable algorithms for rigid body dynamics that exactly preserve energy and momentum. *Int. J. Numer. Meth. Engng.*, **31**, 19–52, (1991).

[12] S. Krenk. A vector format for conservative time integration of rotations. *MULTIBODY DYNAMICS 2007, ECCOMAS Thematic Conference*, C.L. Bottasso, P. Masarati, L. Trainelli (eds.), Milano, Italy 25–28 June 2007.

[13] O. Gonzalez. Mechanical systems subject to holonomic constraints: Differential-algebraic formulations and conservative integration. *Physica D*, **132**, 165–174, (1999).

[14] E.V. Lens, A. Cardona, M. Geradin. Energy preserving time integration for constrained multibody systems. *Multibody Syst. Dyn.*, **11**, 41–61, (2004).

[15] P. Betsch, S. Uhlar. Energy-Momentum conserving integration of multibody dynamics. *Multibody Syst. Dyn.*, **17**, 243–289, (2007).